Applications of Advanced Process Control Techniques to an Italian Water Distribution Network

Applications of Advanced Process Control Techniques to an Italian Water Distribution Network

Silvia Maria Zanoli, *Member, IEEE*, Crescenzo Pepe, Giacomo Astolfi and Lorenzo Orlietti

***Abstract*—In this paper an application of Advanced Process Control techniques to an Italian water distribution network is presented. Several in-depth hydraulic studies had previously been conducted in order to perform hardware modifications through sectorization procedures. In order to further improve performance, both pressure management of the water distribution system and optimization of pump scheduling problems have been addressed. Net pressure has been minimized through two-layer Model Predictive Control techniques, while advanced logics have been designed for the pumps scheduling. The developed Advanced Process Control system has been successfully installed allowing to reduce water losses and to achieve a significant reduction of operational costs in terms of electric energy and fault rates.**

***Index Terms*—Water Distribution Network, Pump Scheduling, Pressure Predictive Control, Energy Efficiency.**

I. INTRODUCTION

WATER Distribution Networks (WDNs) are complex systems generally composed of a large number of interconnected elements such as reservoirs, pipes, pumps, valves and other hydraulic elements. The presence of different conflicting objectives, e.g. fulfilling customers' water demand versus the minimization of energy consumption and water losses/leakages, represents an interesting challenge in the management of WDNs. The development of Advanced Process Control (APC) systems applied to WDNs is clearly within the scope of smart cities, a concept that has become more and more popular in scientific literature and international policies [1]; in [2], a smart city is defined as a city that by monitoring and integrating the conditions of all of its critical infrastructures, including roads, airports, seaports, water, energy power, can better optimize its resources, plan its preventive maintenance activities, and monitor security aspects maximizing also services to its citizens.

Typically, a considerable number of pumps are used to convey water into elevated reservoirs from which the consumer demand is supplied. The high consumption of electrical energy associated with pumping activities, constitutes the largest expense for water utilities. In order to reduce costs and save energy consumption many researchers have focused on the problem of improving the pump scheduling for water distribution systems (WDS).

The pump scheduling problem has been tackled with many different approaches: in [3], a linear programming (LP) optimization problem is formulated and solved for a single tank system for optimal pump scheduling in order to minimize energy cost while in [4] a nonlinear programming-based branch and bound method, and a mixed integer linear relaxation of the original nonconvex formulation is considered. A geometric programming (GP)-based model predictive control (MPC) algorithm, designed to solve the water flow equations and obtain WDN controls, i.e., pump/valve schedules alongside heads and flows is proposed in [5] while in [6] optimal water flow task is formulated as a mixed-integer non-convex problem incorporating flow and pressure constraints, critical for the operation of fixed-speed pumps, tanks, reservoirs, and pipes.

Another significant problem that often has to be dealt in WDNs is represented by water loss: this phenomenon has non-negligible social and economic impacts [7]. For this reason, the detection, prevention and prediction of water losses are topics under the attention of the research community aiming at their avoidance or at least their reduction. Water losses are total losses and comprise real losses and apparent losses. Real losses are losses caused by leakages from bursts in pipes, at network fitting and joints, leakage through service reservoir floors and walls as well as from reservoir overflows whereas apparent losses are mainly due to illegal water consumption and metering errors [8], [9], [10]. Real losses are usually the major part of the water losses.

A leakage detection and isolation method is proposed in [11]: exploiting Barcelona network calibrated model, the resulted pressure estimations are compared to the real measurements, detecting the significant discrepancies. An optimal sensor placement methodology has been applied based on the pressure sensitivity matrix to the leakage presence in the network; the obtained optimization problems are solved through a genetic algorithm. An approach for the localization of leaks is proposed in [12]: pressure sensors alongside a calibrated hydraulic model are used and a differential evolution algorithm solves the leakage localization.

The tied relationship between water losses and operational pressure in WDNs has been proven in different research works [13], [14]. In [15], it was addressed the modelling of leakage and pressure management. It has been shown that high pressure leads to increased water loss and to pipe damages. A real time pressure control methodology for leakage reduction by pressure

Manuscript submitted on March 2021.

S. M. Zanoli and C. Pepe are with the Università Politecnica delle Marche, Ancona (AN), Italy (e-mail: s.zanoli@univpm.it).

G. Astolfi and L. Orlietti are with Alperia Green Future, Falconara Marittima (AN), Italy (e-mail: giacomo.astolfi@alperia.eu).

control valves is presented in [16], [17].

The potential of Model Predictive Control (MPC)-based approaches in WDNs has been proven in different research works. In particular, in [18] a distributed MPC approach designed to work in a cooperative manner for controlling flow-based networks showing periodic behaviors is proposed. Local controllers cooperate in order to enhance the performance of the entire flow network avoiding the use of a coordination layer; this approach has been tested on Barcelona case study. A health-aware MPC that includes an additional goal to extend the components and system reliability has been proposed in [19]: the MPC model uses an extra parameter varying equation that considers the control action as a scheduling variable. A small part of a real water network is used as a case study for illustrating the performance of the proposed approach. Non-linear economic MPC of WDNs is proposed in [20]: a nonlinear hydraulic model is exploited and a simulator is used for online simulation experiments. A new model predictive control strategy based on Gaussian Process for propagating the disturbance forecast uncertainty into the system states is presented in [21].

From literature it is now largely recognized that an effective pressure management of water distribution network is a key point to achieving minimization of the system leaks while maintaining the levels of service required to provide water to the consumers [7]. The pressure management aims at minimizing unnecessary excessive pressure in some areas and at certain times without having to resort to costly replacement work on the network. In this way the problem is not eliminated but its effects are contained to acceptable values with the result of lengthening the average lifetime of the infrastructures. Furthermore, the application of pressure management policies has been demonstrated to pursue additional benefits, such as extending infrastructure life through reduction of the frequency of burst pipes and possibly saving water through reduction of consumption by users in case of pressure dependent demand [22], [23].

This paper describes a project aimed at the optimization of a subnet of a WDN located in Trento (Italy). Two distinct phases have characterized the project: the first phase has been focused on the creation of District Metered Areas (DMAs) within the WDN while the design and installation of an Advanced Process Control (APC) system have been performed in the second phase. The APC system aims to improve the energy efficiency of the subnet through an automatic and smart management of the pumping stations involved, while minimizing the average pressure of the DMA under consideration. The paper focuses mainly on the advanced control aspect. The proposed average pressure minimization strategy is based on a two-layer MPC scheme that handles model uncertainties through a deadbeat Kalman filter. According to the authors' knowledge, this approach is innovative in WDNs field. In addition, tailored control strategies ("move suppression" factors and smart policies for process constraints handling) have been applied for the proposed pump stations scheduling algorithm which result innovative in WDNs pump scheduling applications. The paper extends the results presented in [24]. An in-depth literature review has been added and the developed theoretical formulation has been detailed highlighting the innovation of the proposed methodological approach. New field results have been provided and certified energy savings are shown. The benefits of the recent results achieved in terms of losses and reduction of faults are reported. The paper is organized as follows: Section II describes the APC formulation together with the methodological approach and the innovative contributions with respect to the literature. Section III describes the considered WDN, the network sectorization focusing on the subnet that has been optimized. The algorithm for automatic and smart management of the pumping stations is reported in Section IV, while Section V describes the developed MPC scheme that minimizes the DMA pressure. Field results are reported in Section VI and conclusions are summarized in Section VII.

II. Problem Statement

In the present section, the controllers' formulation has been reported. The overall Advanced Process Control (APC) architecture is described together with the methodological approach adopted and its innovative contributions with respect to the literature.

The water subnet (see Fig. 1) consists of various tanks managed by pumps located in different pumping stations and an urban (valley) district that generates water demand. The flow of water to the district is regulated through a valve (Section III).

The main goals of the APC system are the optimal scheduling of the switching on and off of the water pumps and the minimization of the valley floor pressure. Being a multivariable and constrained control task, for a human operator, to ensure the correct pressure behavior at critical nodes and inside the pipes, maintaining the level of the tanks at the desired values also exploiting natural energy sources (e.g. photovoltaic energy), and smartly switching the pumps of each pumping station, is a non-trivial task.

Pressure management is mainly intended to the water leakages reduction (see Section V) while pumping operations should preferably be concentrated during the daytime hours in order to make the most profit from the electricity produced by the photovoltaic field (see Section IV). Two main control modules characterize the APC system: a pump scheduling module (red rectangle in Fig. 1) and a pressure management MPC module (light blue rectangle in Fig. 1). The dynamic behavior of the overall process consisting of the pumping stations and the urban (valley) district allowed the control problem to be split.

A. Pump scheduling module

As shown in Fig. 1, the water subnet is characterized by different pumping stations. In order to optimize each pumping station, an ad hoc scheduling algorithm for each pumping station has been designed. In this section the basic concepts and ideas are reported. Section IV describes the details of the case study together with two examples of customization.

The algorithm is not formulated as a classical optimization problem, but it is characterized by an advanced rule-based multivariable formulation. The algorithm must compute the number of pumps to be switched on/off and select the specific pumps. The target of the algorithm is the maximization of the pumps' lifetime, the minimization of the pumps' maintenance costs, while maximizing the use of natural energy sources (e.g. photovoltaic energy) and minimizing the electricity demand.

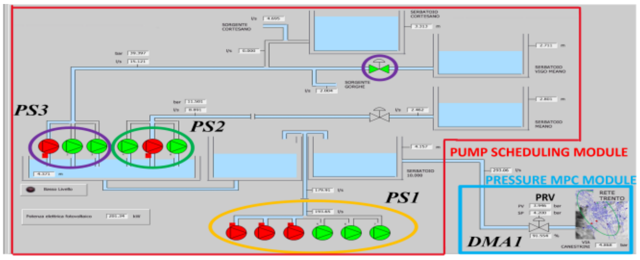

Fig. 1. Scheme of APC system.

The optimality in the process conduction is ensured by the algorithm formulation which finds the most profitable solution taking into account all the significant process variables and all the critical process constraints. This is also made possible by the introduction of "move suppression" factors, specifications ranking, and online calculation of pumps' on/off priorities. The electricity saved represents an example of optimality metric that is exploited to prove the quality of each derived schedule (see Subsection VI.D).

The pump scheduling module has been equipped with suitable minimum and maximum number of switched on pumps to be guaranteed in order to avoid high pressure on the pipes. Together with the fulfilling of the minimum and maximum number of switched on pumps, this module has to preserve from the violation of the maximum value admitted for the lifting pressure (related to the pipes that link each pumping station with the related tank/tanks). The pump scheduling module must manage the switched-on pumps of each pump station in order to respect the upper constraint related to the lifting pressure. Furthermore, the module must guarantee that the level of each tank violates, as little as possible, the imposed safety constraints. Together with the level safety constraints, a set of constraints have been defined which are contained within the safety constraints: they have been named *tube-constraints,* due to the shape of the constraints. Their use will be clarified in Section IV. All physical specifications have been obtained through extended process studies and InfoWorks WS [25] software simulations.

A set of ad hoc specifications has been added to the previously cited specifications in order to increase the pumps' lifetime and to minimize the pumps' maintenance costs. A constraint strictly imposes that a pump switches on can be performed only if a minimum time since last switch on has been elapsed.

In order to increase the robustness of the proposed scheduling algorithms, a set of "move suppression" factors (from an optimal control theory point of view) has been defined for each pumping station. These parameters aid to contain the controller moves and act on the activation of the level *tube-constraints*. The tuning of these parameters has been optimized based on the tanks geometry and on the mean in/out flow rates.

Considering the previously described specifications, the generic pumping stations algorithm, at each control instant, is based on the following steps:

- Acquire plant measurements related to the pumping station (e.g. levels, pressures, pumps status, valves status, in/out tank flow rates) through the SCADA (Supervisory Control And Data Acquisition) system.
- Perform bad detection procedures on the acquired plant signals, in order to detect validity limits violation, freezing/rate of change conditions; if bad detection gives positive results, no move is performed by the algorithm at the current control instant (the next steps are skipped) and an alarm is provided.
- Update the uptime (time since last switch on) and the total uptime (total switch on time since algorithm start up) of each pump with an on status.
- Update the downtime (time since last switch off) and the total downtime (total switch off time since algorithm start up) of each pump with an off status. Increase the counter of failed switch on attempts of each pump for which the algorithm requires a switch on (since the previous instant/instants, F) without success, e.g. due to communication problems or to an undetected anomaly.
- Compute, for each pump, a switch on/off priority (Sw_{ON}, Sw_{OFF}), based on the following formulas:

$$Sw_{ON} = Sw_{ON_0} + R - (F \bmod S) \tag{1}$$

$$Sw_{OFF} = Sw_{OFF_0} - R \tag{2}$$

$$R = fix(\frac{M-T}{U}) \tag{3}$$

  where Sw_{ON_0} and Sw_{OFF_0} represent the default on/off priorities of each pump (default value equal to 1, see Subsection IV.A for a customization example), F is the counter previously cited and S is a scaling factor. mod computes the remainder of the division between F and S. M represents the maximum value among the pumps total uptime at current control instant, T is the current total uptime of the considered pump, U is the uptime upper constraint (see Section IV) and fix is the operation that rounds the considered number to the nearest integer smaller than or equal to it.
- Compute the number of pumps to be switched on/off, based on the specifications ranking (see Section IV), on pumps uptime upper constraints (see Section IV) and respecting the minimum time since last switch on. In some cases, in addition, it could be needed that a pump switches off because its uptime violates the uptime upper constraint and it must be replaced by another pump (see Section IV).
- Select which pumps to be switched on/off. The algorithm searches in descending switch on/off priority order. For the definition of the pumps to be switched off, the algorithm first evaluates the uptime upper constraints and then the uptime lower constraints.

According to the authors' knowledge, the proposed pumping stations algorithm is innovative in many aspects. The introduction of "move suppression" factors and of the *tube-constraints* policy was never proposed in the WDNs pump scheduling algorithms. In Section IV, the positioning of the designed algorithms with respect to the classification formulated in [26] on real time controllers for speed pumps used for tank filling has been reported.

B. Pressure management MPC module

For the pressure management, a tailored MPC module has been designed. With respect to the classification formulated in [26] on real time controllers for service pressure regulation, the proposed solution has been applied on field through a remote-control implementation. A cross-fertilization procedure from the industrial world to the WDNs has been attempted i.e. the synthesis of a two-layer MPC scheme [27], [28], [29] based on linear models that exploits process variables feedback possibly through a deadbeat Kalman filter [30], [31], [32], [33]. This approach, according to the authors' knowledge, was never proposed in the WDNs field.

MPC strategy is based on the knowledge of process model [34]. The proposed MPC module exploits empirical data-based input-output linear models which explain the relationship between the process outputs (Controlled Variables (CVs), $y \in \mathrm{R}^{m_y \mathrm{x} 1}$) and inputs. According to MPC theory, inputs have been split in two groups: the Manipulated Variables (MVs, $u \in \mathrm{R}^{l_u \mathrm{x} 1}$) and the Disturbance Variables (DVs, $d \in \mathrm{R}^{l_d \mathrm{x} 1}$). MVs are the measured process inputs that the MPC module can exploit for the satisfaction of the control/optimization specifications. DVs are the measured process inputs that affect the CVs behavior but, according to process specifications, they cannot be manipulated by the MPC module. In Section V the correspondence between CVs, MVs, DVs groups and physical variables of the considered water network will be specified.

The adopted MPC linear model is characterized by the following discrete-time state space formulation:

$$\begin{aligned} \begin{bmatrix} x(k+1) \\ m(k+1) \end{bmatrix} &= \begin{bmatrix} A & B_m \\ 0_{m_y \mathrm{x} n} & I_{m_y \mathrm{x} m_y} \end{bmatrix} \begin{bmatrix} x(k) \\ m(k) \end{bmatrix} + \begin{bmatrix} B_u \\ 0_{m_y \mathrm{x} l_u} \end{bmatrix} u(k) \\ &+ \begin{bmatrix} B_d \\ 0_{m_y \mathrm{x} l_d} \end{bmatrix} d(k) + \begin{bmatrix} w(k) \\ w_m(k) \end{bmatrix} \\ y(k) &= \begin{bmatrix} C_y & C_m \end{bmatrix} \begin{bmatrix} x(k) \\ m(k) \end{bmatrix} + v(k) \end{aligned} \tag{4}$$

In (4), $x \in \mathrm{R}^{n\mathrm{x}1}$ is the state vector, $A \in \mathrm{R}^{n\mathrm{x}n}$ is the process state dynamic matrix, $B_u \in \mathrm{R}^{n\mathrm{x}l_u}$ is the process MVs-to-state matrix, $B_d \in \mathrm{R}^{n\mathrm{x}l_d}$ is the process DVs-to-state matrix, $C_y \in \mathrm{R}^{m_y\mathrm{x}n}$ is the process state-to-output matrix. In Section V, the procedure to determine the process matrices A, B_u, B_d, C_y will be detailed.

In order to face with model uncertainties and sensors noise/errors, in the MPC linear model additional state $m \in \mathrm{R}^{m_y \mathrm{x} 1}$ and unmeasured disturbance variables terms $w \in \mathrm{R}^{n\mathrm{x}1}$, $v \in \mathrm{R}^{m_y \mathrm{x} 1}$ and $w_m \in \mathrm{R}^{m_y \mathrm{x} 1}$ have been included (see (4)). In this way, an offset-free controller is obtained [32], [33]. The terms just described have been included in (4) through suitable matrices $B_m \in \mathrm{R}^{n\mathrm{x}m_y}$ and $C_m \in \mathrm{R}^{m_y\mathrm{x}m_y}$. Finally, $I_{a\mathrm{x}a}$ represents a $(a \mathrm{~x~} a)$ identity matrix while $0_{a\mathrm{x}b}$ represents a $(a \mathrm{~x~} b)$ zero matrix.

To deal with possible partially unmeasured state, model uncertainties and sensors noise/errors, a state estimation problem has to be solved [32]. Assuming that the defined (B_m, C_m) guarantees the observability of the augmented system (4), a $L = [L_x \quad L_m]^T$ such that

$$\left(\begin{bmatrix} A & B_m \\ 0_{m_y \mathrm{x} n} & I_{m_y \mathrm{x} m_y} \end{bmatrix} - \begin{bmatrix} A & B_m \\ 0_{m_y \mathrm{x} n} & I_{m_y \mathrm{x} m_y} \end{bmatrix} \begin{bmatrix} L_x \\ L_m \end{bmatrix} \begin{bmatrix} C_y & C_m \end{bmatrix} \right) \tag{5}$$

is strictly Hurwitz can be achieved. The estimator equation is:

$$\begin{bmatrix} \hat{x}(k|k) \\ \hat{m}(k|k) \end{bmatrix} = \begin{bmatrix} \hat{x}(k|k-1) \\ \hat{m}(k|k-1) \end{bmatrix} + \begin{bmatrix} L_x \\ L_m \end{bmatrix} \left(y(k) - \begin{bmatrix} C_y & C_m \end{bmatrix} \begin{bmatrix} \hat{x}(k|k-1) \\ \hat{m}(k|k-1) \end{bmatrix} \right) \tag{6}$$

Assuming that A is strictly Hurwitz, the following design choices have been performed:

$$B_m = 0_{n\mathrm{x}m_y} \quad C_m = I_{m_y \mathrm{x} m_y} \quad L_x = 0_{n\mathrm{x}m_y} \quad L_m = I_{m_y \mathrm{x} m_y} \tag{7}$$

The filtered disturbance estimate is

$$\begin{aligned} \hat{m}(k|k) &= \hat{m}(k|k-1) + \left(y(k) - C_y \hat{x}(k|k-1) - \hat{m}(k|k-1) \right) = \\ &= y(k) - C_y \hat{x}(k|k-1) \end{aligned} \tag{8}$$

This design assumes that any error $y(k) - C_y \hat{x}(k|k-1)$ is caused by a constant disturbance acting on the output. If w, w_m and v are assumed as zero-mean white-noise disturbances, the designed estimator corresponds to a deadbeat Kalman Filter ([32], [33]) where:

$$Q_w = 0_{n\mathrm{x}n} \quad Q_{w_m} = I_{m_y \mathrm{x} m_y} \quad R_v \to 0_{m_y \mathrm{x} m_y} \tag{9}$$

Based on the described linear model ((4)-(9)), a two-layer MPC strategy has been formulated. At the lower layer, a Dynamic Optimizer (DO) sub-module performs a constrained optimization, computing the MVs value *u(k)* to be supplied to the plant at each control instant *k*. In the quadratic optimization problem that characterizes this sub-module, constraints over the prediction and control horizons and steady state optimal targets need to be properly set. At this purpose, at the upper layer a Targets Optimizing and Constraints Softening (TOCS) sub-module performs a steady-state constrained optimization, searching pressure minimization directions. As a result, TOCS provides to the DO sub-module a steady-state configuration represented by targets and constraints [27].

TOCS and DO formulation approach makes use of the plant dynamics to eliminate the states from the decision variables by expressing them as an explicit function of the current state and future control input (see [34] for details).

TOCS sub-module performs the first constrained optimization, based on a Quadratic Programing (QP) problem. The formulated cost function is:

$$\begin{aligned} V_{TOCS}(k) &= c_u{}^T \cdot \Delta\hat{u}_{TOCS}(k) + \|\Delta\hat{u}_{TOCS}(k)\|^2_{\mathcal{R}_{TOCS}} \\ &+ \|\varepsilon_{y\_TOCS}(k)\|^2_{\rho_{y\_TOCS}} \end{aligned} \tag{10}$$

which has to be minimized with respect to steady state MV moves vector $\Delta\hat{u}_{TOCS}$ and slack variables vector ε_{y_TOCS}, subject to

$$\begin{aligned} &\text{i. } lb_{du\_TOCS} \le \Delta\hat{u}_{TOCS}(k) \le ub_{du\_TOCS} \\ &\text{ii. } lb_{u\_TOCS} \le \hat{u}_{TOCS}(k) \le ub_{u\_TOCS} \\ &\text{iii. } lb_{y\_TOCS} - \gamma_{lby\_TOCS} \cdot \varepsilon_{y\_TOCS}(k) \le \hat{y}_{TOCS}(k) \le \\ &\qquad \le ub_{y\_TOCS} + \gamma_{uby\_TOCS} \cdot \varepsilon_{y\_TOCS}(k) \\ &\text{iv. } \varepsilon_{y\_TOCS}(k) \ge 0 \end{aligned} \tag{11}$$

DO sub-module solves a QP problem, based on the following cost function:

$$\begin{aligned} V_{DO}(k) &= \sum_{j=1}^{m_y} \sum_{i=H_{w_j}}^{H_p} \left(Q_{(j,j)}(i) \cdot \left(\hat{y}_j(k+i|k) - r_j(k+i|k) \right)^2 \right) \\ &+ \sum_{i=1}^{H_p} \|\hat{u}(k+i-1|k) - u_r(k+i-1|k)\|^2_{S(i)} \\ &+ \sum_{i=1}^{H_u} \|\Delta\hat{u}(k+i-1|k)\|^2_{\mathcal{R}(i)} + \|\varepsilon_{DO}(k)\|^2_{\rho_{DO}} \end{aligned} \tag{12}$$

which has to be minimized with respect to MV moves vector $\Delta\hat{u}$ and slack variables vector ε_{DO}, subject to

$$\begin{aligned} &\text{i. } lb_{du\_DO}(i) \le \Delta\hat{u}(k+i-1|k) \le ub_{du\_DO}(i), i = 1, \dots, H_u \\ &\text{ii. } lb_{u\_DO}(i) \le \hat{u}(k+i-1|k) \le ub_{u\_DO}(i), i = 1, \dots, H_u \\ &\text{iii. } lb_{y\_DO_j}(i) - \gamma_{lby\_DO_j}(i) \cdot \varepsilon_{DO}(k) \le \hat{y}_j(k+i|k) \le ub_{y\_DO_j}(i) + \\ &\qquad + \gamma_{uby\_DO_j}(i) \cdot \varepsilon_{DO}(k), \quad j = 1, \dots, m_y, \ i = H_{w_j}, \dots, H_p \\ &\text{iv. } \varepsilon_{DO}(k) \ge 0 \end{aligned} \tag{13}$$

In (10) and (12), $\mathcal{R}_{TOCS}$ and $\mathcal{R}$ weight the magnitude of the MV moves $\Delta\hat{u}_{TOCS}(k)$ and $\Delta\hat{u}(k+i-1|k)$. DO MV moves are computed over a control horizon H_u (in this work H_u=H_p). Pressure minimization directions are guaranteed through c_u positive weight in (10). Hard constraints on MV moves and values are imposed in (11) and (13) through lower and upper bounds terms lb_{du_TOCS}, ub_{du_TOCS}, lb_{u_TOCS}, ub_{u_TOCS}, lb_{du_DO}, ub_{du_DO}, lb_{u_DO}, ub_{u_DO} terms. CVs constraints in (11.iii) and (13.iii) have been considered as soft constraints, and their possible violations are made possible through the introduction of ε_{y_TOCS} and ε_{DO} slack variables vectors. Within these vectors, a set of slack variables has been defined for each CV; the importance of CVs constraints has been defined through $\gamma_{lby\_TOCS}, \gamma_{uby\_TOCS}, \gamma_{lby\_DO}, \gamma_{uby\_DO}$ in (11.iii) and (13.iii) and through ρ_{y_TOCS} and ρ_{DO} in (10) and (12).

In (12), r and u_r represents the targets that are provided to DO by TOCS sub-module. In fact, these optimal targets are not a priori known by engineers/technicians of the considered water network: this has motivated the introduction of the described two-layer MPC architecture.

III. Water Distribution Network Description

The considered WDN refers to Trento, a city located in the north of Italy. The water distribution network spreads in a wide area, forming a total of 676 km of main pipes; it serves local residential users and includes 92 sources, 21 underground aquifers, 65 water tanks and reservoirs. The whole network counts approximately 8000 pipes, 15000 nodes, 69 pumps and 400 valves. Approximately 63% of the water sources are underground aquifers located in the valley floor.

The WDN extends for more than 600 km and it is characterized by freshwater sources, underground aquifers, water tanks and reservoirs. Before designing and installing the APC system, hardware modifications on the WDN have been performed, aimed at the creation of District Metered Areas (DMAs) [35], [36], [37]. Fig. 2 reports the previous WDN pressure distribution, simulated through InfoWorks WS software [25]. Areas characterized by a pressure lower than 2.5 bar (yellow, light-red and red) can be noted, together with areas with a pressure greater than 4 bar (blue, dark blue and purple). The conducted simulations have certified that the WDN was characterized by an excessive pressure in most of its valley floor extension, but essential to serve utilities located at higher altitudes. This called for a sectorization study which at the time of the present project had already been completed, resulting in the creation of separate districts. In Fig. 3 the hydraulic model of the considered DMA is presented together with the Google maps of the corresponding geographic zone. The blue circle shows the geographical location of the principal district uphill reservoir; the main water supplies are located within the red circle while the residential user are within the green circle. Among the many benefits achievable through sectorization, the most interesting effects are the contribution offered to the mitigation of the water losses and the reduction of the maintenance costs [38], [39]. The present paper refers to a subnet that is characterized by one DMA (Fig. 1: *DMA1*) and by three pumping stations (Fig. 1: *PS1*, *PS2*, *PS3*). *DMA1* represents the bottom of the valley of Trento. The tank that is filled by *PS1* supplies water to *DMA1* and the regulation of the pressure of the pipes between the tank and *DMA1* is performed by a PRV (Pressure Reducing Valve). Furthermore, the tank filled by *PS1* supplies also the tank that supplies *PS2* and *PS3*. *PS2* supplies a single tank while *PS3* supplies two tanks located at different altitudes; *PS3* water flow is regulated by an on/off valve (see Fig. 1).

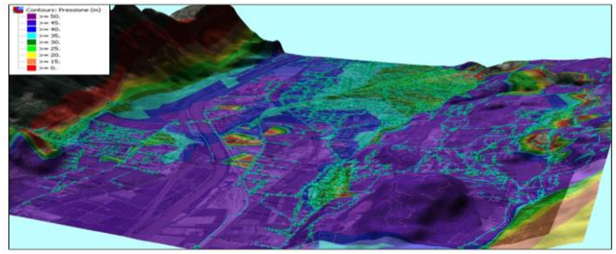

Fig. 2. WDN pressure distribution: the high pressure at the bottom valley called for the creation of DMAs.

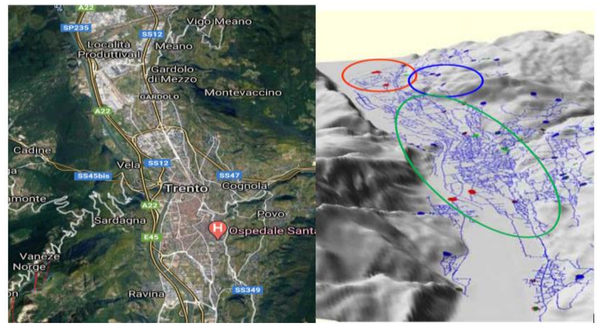

Fig. 3. Google Maps detail of the DMA (left). Hydraulic model of the DMA (right): consumers (green circle), main reservoir (blue circle), water supplies (red circle).

Plant measurements (e.g. water level inside each tank, pressures at critical nodes, flow rates…) are available through remote terminal units which are interrogated with sampling periods characterized by a lower bound. For example, all measurements related to the PRV and to the bottom of the valley of Trento (pressures at critical nodes) are refreshed with a period greater than or equal to 15 minutes. In turn, measurements related to the pumping stations (e.g. water level inside each tank) are refreshed with a period greater than or equal to 2 minutes. As it will be detailed in the next sections, the pump scheduling module runs with a sampling time equal to 2 minutes for all pumping stations while the pressure management MPC module runs with a sampling time of 15 minutes. These settings were based on the previous considerations on measurement refresh and on the physical behavior of the process. In fact, due to the characteristics of the process, and particularly the fact that the tank filled by *PS1* (which supplies water to *DMA1*) has slow dynamics, the timescale difference between the two modules is well-posed.

The developed APC system acquires plant measurements through a SCADA system and bad conditions detection routines (i.e. validity limits, freezing, rate of change) have been implemented in both control problems described below. Thanks to the implemented bad detection procedures, robustness of the overall APC system is ensured with respect to the refreshing of the measurements by the remote terminal units.

IV. Pumping Stations Scheduling Algorithm

The case study of the present paper is characterized by three pumping stations (Fig. 1: *PS1*, *PS2*, *PS3*). In this section the algorithm described in Subsection II.A is focused on the case study. Subsections IV.A and IV.B describe two examples of customization (*PS1*, *PS2*).

The main features of the pumping stations have been reported in Table 1; the minimum and maximum number of switched on pumps to be guaranteed by the APC system have been reported in the third column. The sampling time related to the algorithm of each pumping station has been reported on the fifth column. The sampling time setting has been based on the assigned control specifications and taking into account the time that each pump/valve requires for a switch on/off.

The main features of the tanks supplied by the pumping stations have been reported in Table 2: *PSn* (1) (*n=1,2*) are the tanks supplied by *PS1* and *PS2*, while *PS3* (1) and *PS3* (2) are the tanks supplied by *PS3*.

The maximum value admitted for the lifting pressure (related to the pipes that link each pumping station with the related tank/tanks) has been reported in Table 2. Furthermore, as described in Section II, the following concepts are preferable:

- A pump is switched on only if at least 12 hours (720 minutes) have passed since its last switch off.
- If a pump has been switched on, it is preferable that at least two hours (120 minutes) elapse before switching it off.
- A pump that is switched on remains in the on status (continuously) no more than seven days (10080 minutes).

Table 4 reports the "move suppression" factors that have been defined for each pumping station. Considering *PS1*, the next pump switch on action can only be performed if 30 minutes have passed since last pump switch on action. The counter resets to zero if an isolated pump switch off is performed. The same scheme applies to switch off procedures. The setting parameters for the present pumping station are reported in Tables 1-4 (see algorithm in Subsection II.A).

Considering formulas (1)-(3), U is the uptime upper constraint reported in Table 3. The specification ranking used for the computation of the number of pumps to be switched on/off is reported in Table 5 (a lower ranking number represents a higher priority). Note that the specifications reported in Table 5 require either a switch on action or a switch off action. In some cases, in addition, a pump may need to be switched off because its uptime violates the imposed uptime upper constraint and must be replaced by another pump.

With respect to the classification formulated in [26] on real time controllers for speed pumps used for tank filling, a two-point control logic based on multiple fixed trigger levels has been designed for *PS3* (see level safety constraints and level *tube-constraints* in Table 2). *PS1* control algorithm exploits a two-point control logic with fixed trigger levels (see level safety constraints in Table 2) and variable trigger levels (see level *tube-constraints* in Subsection IV.A). Finally, *PS2* control algorithm replicates the *PS3* controller extending it to variable speed pumps (see Subsection IV.B).

Table 1. Pumping stations main features.

Pumping Station	Pumps Available	Min-Max Switched On Pumps	Valves Number	APC Sampling Time [*min*]
PS1	6	1-4	0	2
PS2	3	0-2	0	2
PS3	3	0-1	1	2

Table 2. Tanks main features.

Tank	Safety Constraints [*m*]	Tube Constraints [*m*]	Pressure Constraints [*bar*]
PS1 (1)	2.5-5	see III.A	not defined
PS2 (1)	2.5-3.1	2.7-2.8	0-25
PS3 (1)	2.9-3.3	3-3.1	0-60
PS3 (2)	1.5-3.25	2.7-2.7	

Table 3. Pumps time constraints.

Pumping Station	Downtime Lower Constraint [*min*]	Uptime Lower Constraint [*min*]	Uptime Upper Constraint [*min*]
PS1	720	120	10080
PS2	10	10	1440
PS3	10	10	1440

Table 4. Pumps "move suppression" time constraints (min).

Pumping Station	*PS1* [*min*]	*PS2* [*min*]	*PS3* [*min*]
Tube Sw. On/Off	30/90	45/not defined	not defined

Table 5. Specifications ranking.

Specification	Ranking
Min-Max Switched On Pumps	1
Pressure Constraints	2
Safety Constraints	3
Photovoltaic power Saturation	4
Tube-Constraints	5

A. PS1 scheduling customization

PS1 is characterized by six pumps (1, 2, 3, 5, 6, 7) as shown in Table 1. Underground aquifers supply water to these pumps and each pump requires 75 kW power. During the project, a photovoltaic field (253 kW) has been assembled: the presence of a photovoltaic field represents an important feature that creates a conflict with the common management of a pumping station. In fact, if a photovoltaic field is not present, the only economic aspect to be taken into account is represented by the energy price in the different hours of a day: often, it is preferable to fill the tanks during the night. In order to preserve this feature, *tube-constraints* have been suitably defined for the different days of each week within each season, taking into account water scheduling demand. Due to the presence of the photovoltaic field, the algorithm tries to guarantee that the overall energy provided by the field is always saturated (see Table 5). Pumps #2 and #7 are characterized by automatic discharge. For this reason, it is preferable to have a greater number of switch on/off action on these pumps, in order to limit the side effects of a pump status switch. In order to guarantee this important aspect, Sw_{ON_0} and Sw_{OFF_0} parameters (see (1), (2)) related to pumps #2 and #7 have been set greater with respect to the other pumps.

B. PS2 scheduling customization

As can be noted in Table 1, *PS2* is characterized by three pumps (4, 5, 6). Pumps #4-5 are equipped with an on/off command and only one at a time can be in an on status. When either pump #4 or pump #5 is in an on status, a level PID controller acts (the related set-point is about 3 m and it is not managed by *PS2* module). Pumps #4-5 are equipped with an inverter and the related current motor speed (Hz) is a known information. Pump #6 is an on/off pump and it can be switched on if necessary, to maintain the tank within admissible bounds. Pump #6 can be switched on only if also either pump #4 or pump #5 already is in an on status. In order to smartly manage the pump station, ad hoc safety and *tube-constraints* have been defined (see Table 2). Furthermore, a zone of inverter normal operation has been identified when either pump #4 or pump #5 is in an on status (e.g. 44 Hz-47 Hz). When either pump #4 or pump #5 is in an on status and the related inverter is in the cited operating zone, the *tube-constraints* are not considered by *PS2* module. The *tube-constraints* activation takes place when the inverter violates the upper/lower bound of the normal operation zone; in this case, *PS2* module can switch on/off pump #6 accordingly to the *tube-constraints*. When pump #6 is switched on, the inverter lower bound is automatically changed to 60 Hz in order to always enable its switch off in case of *tube* upper constraint violation.

V. Pressure MPC Strategy

As reported in Section III, the regulation of the pressure of the pipes between the *PS1* tank and *DMA1* is performed by a PRV (Pressure Reducing Valve). The PRV pressure set-point represents the MV of the proposed MPC strategy. The main CVs are pressures at critical nodes of *DMA1*. The DVs are the flow rates toward and from *DMA1* with respect to other DMAs, since the MPC module cannot modify them (see Subsection II.B): other external control units manipulate them.

A data-based modelling approach has been adopted, as the available physical model was not suitable for real-time pressure control. An ad hoc data collection phase was designed in order to capture the most significant dynamics on the pressure at critical nodes of the *DMA1* district; step test procedures have been executed on the process, suitably acting on inputs (u, d). Exploiting step test data, for each input-output pair (i.e. for each MV-CV and DV-CV pair), a first-order plus deadtime model (asymptotically stable) has been considered and suitable parameters' values have been identified [40]; in equation (14) the parametric expression of each model in Laplace domain is reported.

$$M(s) = \frac{K}{Ts+1} e^{-T_d s} \tag{14}$$

where K is the steady state gain, T is the time constant and T_d is the dead time (or delay) of the input-output channel. Table 6 reports the gain values K of some of the models obtained in the identification phase. Note the different signs in Table 6: for example, DV4 represents a water lift toward another *DMA* that decreases the pressure at critical nodes and this is explained by the negative value. The linear model represented by the Multi-Input Multi-Output (MIMO) transfer function matrix, obtained from the identification phase (see (14)), has been validated based on typical metrics (e.g. goodness of fit statistics, residual analysis and confidence and prediction bounds). Considering the MIMO transfer function matrix, a continuous-time state space realization [41] has been firstly computed. The state vector resulting from a state space realization procedure has not a physical meaning. The state-space description provides the dynamics as a set of coupled first-order differential equations in a set of internal variables (state variables), together with a set of algebraic equations that combine the state variables into physical output variables [41]. Successively a discretization procedure has been performed, using a zero-order hold and a suitable sample time; the input-output delays have been included in to system dynamics [42]. Finally, the process matrices A, B_u, B_d, C_y of equation (4) have been obtained. The predictions provided by the linear model (4), enriched with estimator (6) under the assumptions (5), (7) and (9), provided adequate performances. The proposed deadbeat Kalman filter, tailored for handling model uncertainties, guarantees suitable feedback exploitation. Furthermore, in order to deal with the process nonlinearities and to preserve the controller performances, the models are periodically revised during the project maintenance.

Table 6. u-y and d-y transfer function gain signs.

Process Var	**MV1** [*bar*]	**DV1** [$l \cdot s^{-1}$]	**DV2** [$l \cdot s^{-1}$]	**DV3** [$l \cdot s^{-1}$]	**DV4** [$l \cdot s^{-1}$]	**DV5** [$l \cdot s^{-1}$]
CV1 [*bar*]	+ 0.8000	+ 0.0057	+ 0.0001	+ 0.0097	- 0.0130	
CV2 [*bar*]	+ 0.5000	+ 0.0057	+ 0.0001	+ 0.0097	- 0.0300	
CV3 [*bar*]	+ 0.4800				- 0.013	+ 0.0079
CV4 [*bar*]	+ 0.7000	+ 0.0031		+ 0.0031	- 0.015	
CV5 [*bar*]	+ 0.9978					
CV6 [*bar*]	+ 0.5500	+ 0.0057	+ 0.0003	+ 0.0019	- 0.015	

Table 7. Grouping policy for CVs constraints relaxation.

Constraints group rank	Process Variables
1	{CV4, CV6}
2	{CV1, CV2, CV3, CV5}

As described in Section III, plant measurements related to the PRV and to the bottom of the valley of Trento are refreshed with a period greater or equal to 15 minutes. For this reason, the MPC algorithm sampling time has been set to 15 minutes. The prediction horizon H_p has been set to 5 steps (75 minutes) based on the system dynamics.

PRV pressure set-point constraints (i.e. MV constraints in (11) and (13)) are set based on physical manufacturing limitations of the valve and on its dynamics. The constraints of the pressures at critical nodes of *DMA1* (i.e. CV constraints in (11) and (13)) are set considering the sectorization works and the insights gained by the InfoWorks WS [25] software simulations.

Table 7 reports the adopted policies for constraints relaxations (see 12.iii) and 14.iii)): CVs have been classified in two different groups. Group 1 includes variables that are more crucial with respect to group 2 variables. The two controlled pressure CV4 and CV6 (see Table 6) share the same rank and have been defined as the most important CVs, because they represent the most critical pressure nodes in the considered DMA.

VI. Results

Fig. 4 and Fig. 5 show the Graphical User Interface (GUI) of the *PS1* module and of the pressure MPC module, respectively. It can be noted the presence of on-off buttons which allow disabling the APC control on each pump and each pressure MV-CV. Furthermore, in order to guarantee a smart monitoring, all anomalies and bad conditions are notified to plant operators. From GUI, operators can monitor the uptime, downtime, total uptime and total downtime of each pump, together with the total number of switching on/off. In addition, an online explanation of the algorithm' decision logics is provided. This feature is greatly appreciated by the operators.

In Subsections VI.A-C significant examples of the APC performance are reported. Subsection VI.D reports energy saving and benefits results.

A. PS1 examples

In this section various interesting situations related to the *PS1* pumping station are analyzed and the *PS1* module performances are commented. In Fig. 6, it can be noted that, in the morning, the water level (blue line) is within the safety constraints (red dashed lines) but is violating the tube upper constraint (green dashed line). There are three pumps with on status (light green line) and the photovoltaic power (dark green line) is greater than 150 kW. Note that in Fig. 6 and in all the following, the photovoltaic power is normalized by a factor of 75 for a better graphical representation. Remember that, as described in Subsection IV.A, each pump of *PS1* station requires a nominal power of 75 kW. A conflict between the *tube-constraints* (soft constraints) and the saturation of the photovoltaic power (see Table 5) occurs: the *tube* upper constraint requires one pump to be switched off, while the photovoltaic power, in order to remain saturated, requires to keep the status of the pumps unchanged. Due to the higher priority of the photovoltaic power over the *tube-constraints,* the *PS1* module does not perform any control action thus keeping the status of each pump unchanged. Another interesting situation is depicted in Fig. 7. The tank level (blue line) on June 1st 2020 at 05:42 am, is respecting the safety constraints (red dashed lines) and starts violating the *tube* upper constraint (green dashed line). At this time instant, there are four pumps on (light green line) and the photovoltaic power production (dark green line) is about zero. Since no other control specification (see Table 5) ranked with a higher priority is active, in this situation, the *PS1* module decides to switch off a pump in order to satisfy the *tube* upper constraint. Since at the analyzed instant, all the pumps have the same switch-off priority values, the *PS1* module switches off pump #5 (see Fig. 8) as it has been active for longer (see Fig. 9). In Fig. 8 (and in the following Fig. 15 and Fig. 19) nonzero values indicate pumps that are switched-on. Then, at 11:40 am of the same day, the tank level while respecting the safety constraints, starts violating the *tube* lower constraint. At this time, there are three pumps that have on status (light green line) and the photovoltaic power (dark green line) is greater than 150 kW. In this situation, the *PS1* module switches on one pump in order to satisfy the *tub*e lower constraint specification, and given that no other control specification (see Table 5) ranked with a higher priority is active. *PS1* module switches on pump #1 (see Fig. 8), based on the computed switch-on priority. Since at the analyzed instant all switch-on priority values of the pumps are the same, *PS1* module selects pump #1 given its longer downtime status (see Fig. 10). Then, on June 2nd 2020 at 07:12 am, the tank level

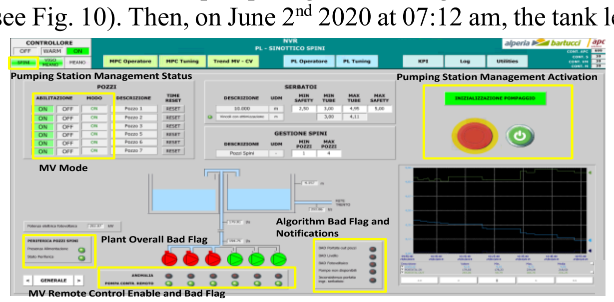

Fig. 4. GUI of *PS1* module (main page).

Fig. 5. GUI of pressure MPC module.

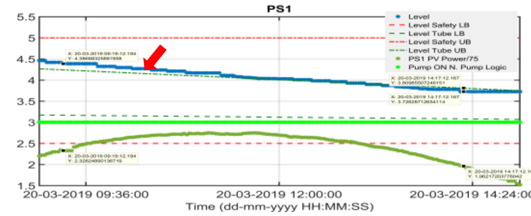

Fig. 6. *PS1* example: saturating the photovoltaic power.

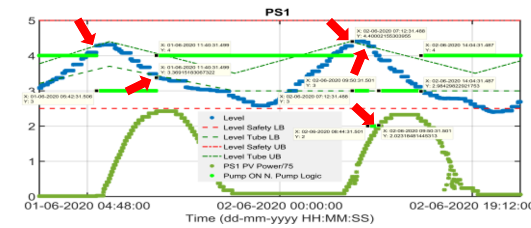

Fig. 7. *PS1* example: controlling the *tube-constraints* and saturating the photovoltaic power (level and photovoltaic power).

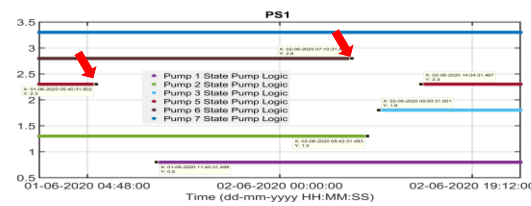

Fig. 8. *PS1* example: controlling the *tube-constraints* and saturating the photovoltaic power (pump status).

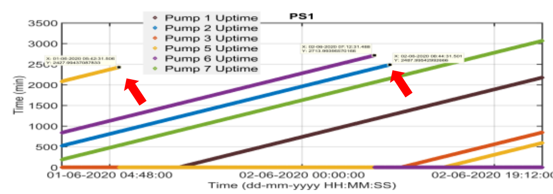

Fig. 9. *PS1* example: controlling the *tube-constraints* and saturating the photovoltaic power (pump uptime).

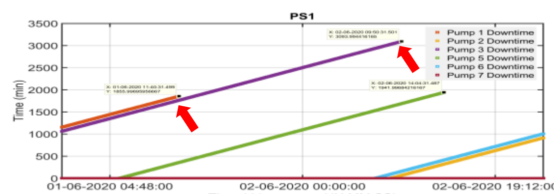

Fig. 10. *PS1* example: controlling the *tube-constraints* and saturating the photovoltaic power (pump downtime).

is respecting the safety constraints and starts violating the *tube* upper constraint. At this moment, there are four pumps with on status and the photovoltaic power is lower than 75 kW. In this situation, *PS1* module decides to switch off one pump, i.e. pump #6, in order to satisfy the *tube* upper constraint, the choice been based on the same logics discussed previously (Fig. 8-9). It can be noted that the tank level is still violating its *tube* upper constraint but no further action is undertaken before 08:44 am. At this moment, the “move suppression” factors specification (see Table 4) is no longer active, since at least 90 minutes have been passed from the last pump switch off action; furthermore, at this time, the photovoltaic power is lower than 150 kW, so *PS1* module can reduce the number of switched on pumps up to two. *PS1* module switches off pump #2, based on the same logics previously described (see Fig. 8-9). Finally, at 09:50 am,

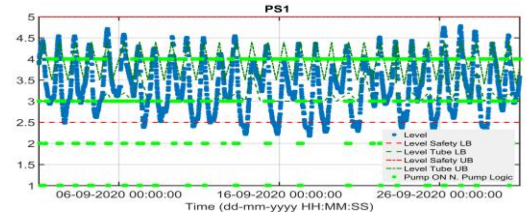

Fig. 11. *PS1* example: monthly performance (level).

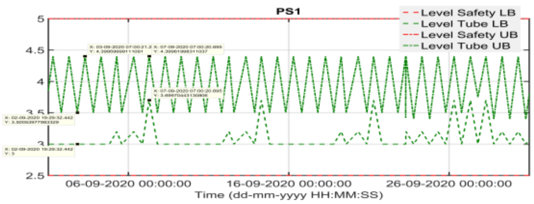

Fig. 12. *PS1* example: monthly performance (constraints).

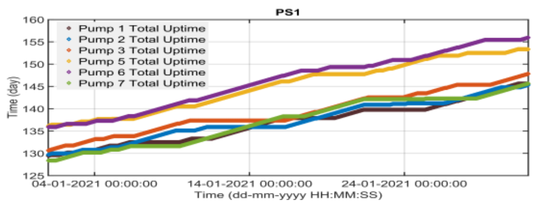

Fig. 13. *PS1* example: long time performance (pump total uptime).

Table 8. *PS1* example: long time performance (pump total uptime detail).

PS1 Pump	#1	#2	#3	#5	#6	#7
Total Uptime [*day*]	146	145	148	153	156	146

the photovoltaic power exceeds 150 kW: three pumps with on status are possibly required, so *PS1* module switches on one pump. According to the same logics previously described (Fig. 8, Fig. 10) pump #3 is switched on.

Fig. 11-12 report an example of monthly performance related to the tank level. As can be noted in Fig. 11, *PS1* module drives the pump scheduling to optimized conditions, thanks to an intelligent variable *tube-constraints* set-up (Fig. 12). The tank level (Fig. 11, blue line) never violates the safety upper constraint and the relaxations of the safety lower constraint are negligible. Fig. 13 reports the total pump uptime performance related to nine months of activity of *PS1* module. As can be noted, the pumps utilization is adequately balanced. Table 8 reports the detailed data.

B. PS2 examples

In this section various interesting situations related to the *PS2* pumping station are analyzed and the *PS2* module performances are commented. In Fig. 14 it can be noted that, on June 22nd 2020 at 06:24 am, the level (blue line) is respecting the constraints (red dashed lines) but is violating the *tube* lower constraint (green dashed line). At that instant, there is no pump with an on status (light green line). In this situation, *PS2* module decides to switch on one pump in order to satisfy the *tube* lower constraint, given the current inactivity of the specifications (see Table 5) that are ranked with higher priority. When no pump is in on status, *PS2* module can only switch on either pump #4 or pump #5 (i.e. motorized pump). *PS2* module decides to switch on pump #4 (see Fig. 15), based on the computed switch-on priority. Since at the analyzed instant, all switch-on priority values are the same, *PS2* module selects pump #4 because its downtime is longer (see Fig. 16). When pump #4 is switched on, its PID level controller starts to regulate the level to a set-point equal to 3 m (Fig. 17). In the time period 06:24 am-07:10 am the tank level is violating its *tube* lower constraint and the pump #4 inverter (Fig. 17, pink line) is violating the upper bound of its normal operation zone (Fig. 17, ochre line). At 07:10 am, the "move suppression" factors specification is satisfied (see Table 4), i.e. at least 45 minutes have been passed from the last pump switch on action. Thus, in order to support the level PID controller action of pump #4, *PS2* module decides to switch on pump #6 (i.e. the only available pump in this condition). When pump #6 is switched on, the pump #4 inverter lower bound is automatically changed to 60 Hz (Fig. 17, green line) in order to always enable its switch off in case of *tube* upper constraint violation. This violation takes place at 07:56 am (Fig. 14): *PS2* module switches off the pump #6 (Fig. 15). At 11:54 am (Fig. 14) the tank level, is still violating its tube upper constraint and the pump #4 inverter (Fig. 17, pink line) is violating the lower bound of its normal operation zone (Fig. 17, green line): *PS2* module decides to switch off pump #4 (Fig. 15). Fig. 18 reports total pump uptime performance related to one month of *PS2* module activity. Pumps #4 and #5 utilization is balanced and pump #6 has a very low total uptime since it has been defined "auxiliary pump". Table 9 reports pump total uptime over a period of nine months.

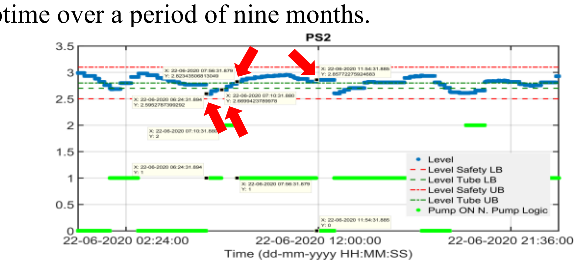

Fig. 14. *PS2* example: controlling the *tube-constraints* (level).

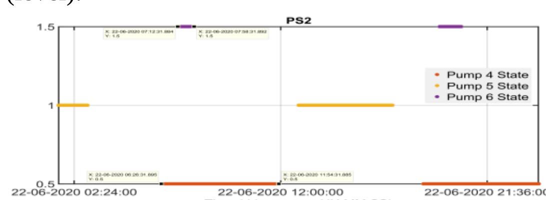

Fig. 15. *PS2* example: controlling the *tube-constraints* (pump status).

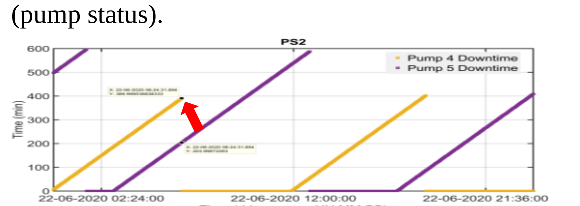

Fig. 16. *PS2* example: controlling the *tube-constraints* (pump downtime).

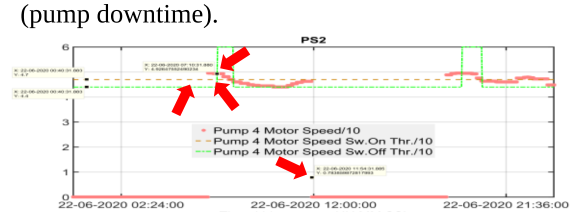

Fig. 17. *PS2* example: controlling the *tube-constraints* (pump motor speed).

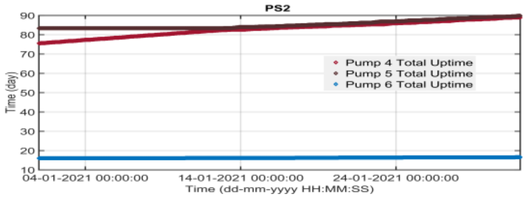

Fig. 18. *PS2* example: long time performance (pump total uptime).

Table 9. *PS2* example: long time performance (pump total uptime detail).

PS2 Pump	#4	#5	#6
Total Uptime [*day*]	89	90	17

C. DMA1 pressure MPC examples

Fig. 19-21 represents two operational days of the *DMA1* District Metered Areas controlled by the MPC module. The most critical process variables (CV4 and CV6, Fig. 19-20) are shown, together with the MV (PRV pressure set-point, Fig. 21). As can be seen, the controller performs differentiated actions during daytime periods versus nighttime periods, based on the behavior of the CVs. On daytime periods (see cyan circles in Fig. 19-21) the controller moves the PRV pressure set-point (Fig. 21) in order to keep the CVs within the assigned constraints (Fig. 19-20, red dashed lines) and often the MV saturates its upper constraint (Fig. 21). On night periods (see black circles in Fig. 19-21), due to the increase of the pressures at critical nodes, the controller decreases the MV.

Fig. 22-23 show an example of the robustness and safety of the proposed MPC scheme with respect to signal bad conditions. For a period of about one hour, plant measurements related to the pressure at critical nodes (see, for example, CV6 in Fig. 22) do not update (freezing condition): the MV (see Fig. 23) safely does not move remaining at a value equal to 4 bar.

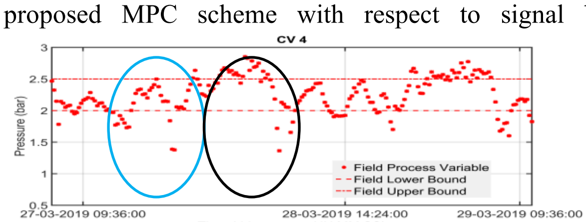

Fig. 19. *DMA1* pressure MPC (CV4).

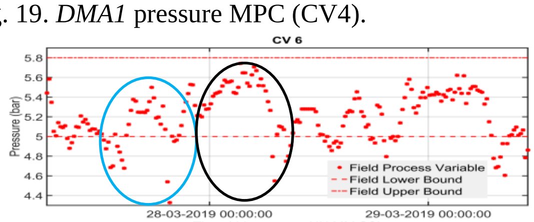

Fig. 20. *DMA1* pressure MPC (CV6).

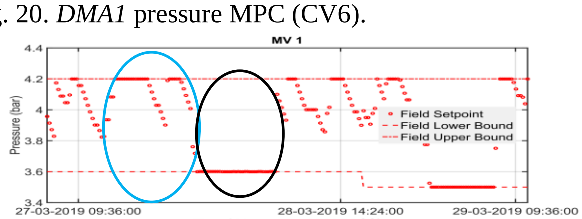

Fig. 21. *DMA1* pressure MPC (MV1).

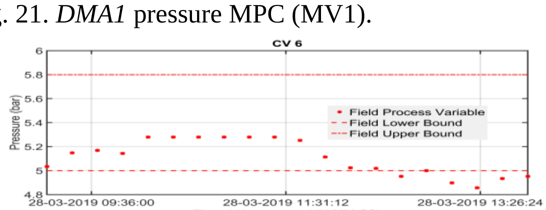

Fig. 22. *DMA1* pressure MPC, CVs freezing (CV6).

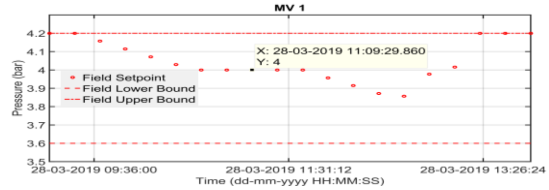

Fig. 23. *DMA1* pressure MPC, CVs freezing (MV1).

D. Global results

The project described in the present paper began in 2017. The sectorization works were completed in December 2018 and the overall APC system has been installed on the real plant in March 2019. The control design choice that motivated the proposal of the described APC system as a substitute of human operated control or basic decoupled Single-Input Single-Output (SISO) process controllers, proved successful in dealing with the WDN multivariable and constrained subnet. Furthermore, the need to anticipate critical control actions, has called for predictive control approaches. The APC system has obtained the Industry 4.0 compliance certification. Up to now, the service factor of the APC system is greater than 95%. Table 10 reports 2019-2020 saving and benefits related to *DMA1* project. BAC (Billed Authorized Consumption) represents the billed water related to *DMA1* (about 63% of the total water). Thanks to the developed project, a significant reduction of the average pressure with respect to the defined baseline (about 5.2 bar) has been achieved, as can be noted also in Fig. 24. In particular, 2.75% (2019) and 4.67% (2020) pressure reduction has been obtained. The obtained pressure reduction led to a significant loss reduction, as shown in Fig. 25. The overall pressure reduction allowed to reduce the load stress of the *DMA1*: this fact has been proven by additional significant fault reduction

Table 10. Global results: 2019-2020 savings and benefits.

	2019	2020
BAC (Billed Authorized Consumption) [m^3]	6700000	
Water saved [m^3]	81474.46	136875.29
Electricity saved [*kWh*]	28480.26	52842.49
kg CO2 equivalents avoided [$kgCO_2$]	8770	16280
tep [*tep*]	5.33	9.88
Pressure reduction [%]	2.75	4.67
Loss reduction [%]	5.43	9.13

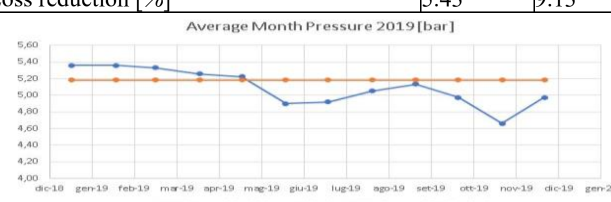

Fig. 24. Global results: 2019 average monthly pressure.

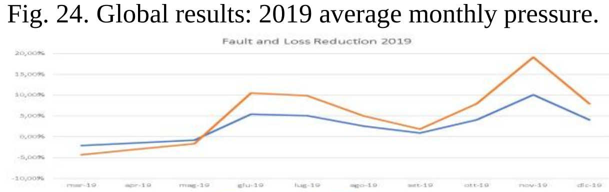

Fig. 25. Global results: 2019 fault ad loss reduction.

that has been registered in 2019 and 2020. Fig. 25 depicts 2019 faults and losses monthly report. Thanks to this result, the maintenance interventions have been significantly reduced. Finally, it is worth to note the significant water saving achieved, along with a substantial reduction in electricity demand.

VII. Conclusions

In the present paper, a project aimed at optimizing a subnet of a Water Distribution Network located in Trento (north of Italy) has been described. The project consisted of two main parts: hardware modifications and Advanced Process Control design. Hardware modifications, represented by sectorization and creation of District Metered Areas, were necessary to achieve the physical conditions for lowering the average net pressure. Among the created districts, the area represented by the bottom of the valley of Trento has been chosen as starting point for the optimization procedure. The Pressure Reducing Valve (pressure) set-point is modulated through an innovative method: a two-layer Model Predictive Control scheme that exploits the pressure measured at critical nodes; model uncertainties are handled through a deadbeat Kalman filter. In addition, three pumping stations of the subnet have been optimized through the creation of a smart and fully automatic scheduling algorithm: the algorithm defines the pumps to be switched on/off based on level constraints and taking into account the price of energy along with free energy sources (photovoltaic field). The selection of the pumps to be switched on/off takes into account the uptime and downtime of pump in order to maximize the pumps' lifetime.

The introduction of "move suppression" factors and of the *tube-constraints* policy represents an innovative aspect in the WDNs pump scheduling algorithms. The overall Advanced Process Control system, composed by the Model Predictive Control and the scheduling algorithm modules, has been successfully installed on the real plant on March 2019. Industry 4.0 compliance certification and a service factor greater than 95% have been obtained. Significant energy efficiency results and benefits have been achieved. Future work will focus on improving process modellization and extending the controller to other districts.

References

[1] V. Albino, U. Berardi, and R.M. Dangelico, "Smart Cities: Definitions, Dimensions, Performance, and Initiatives," *Journal of Urban Technology*, vol. 22, no. 1, pp. 3-21, 2015. DOI: 10.1080/10630732.2014.942092.

[2] R.E. Hall, B. Bowerman, J. Braverman, J. Taylor, H. Todosow, and U. Von Wimmersperg, "The vision of a smart city," in Proc. 2nd International Life Extension Technology Workshop, Paris, FR, 2000.

[3] M.F.K. Pasha, and K. Lansey, "Optimal Pump Scheduling by Linear Programming," in Proc. World Environmental and Water Resources Congress, Kansas City, MO, USA, 2009. DOI: 10.1061/41036(342)38.

[4] G. Bonvin, S. Demassey, and A. Lodi, "Pump scheduling in drinking water distribution networks with an LP/NLP-based branch and bound," *Optim Eng*, vol. 22, pp. 1275-1313, 2021. DOI: 10.1007/s11081-020-09575-y.

[5] S. Wang, A. F. Taha, N. Gatsis, and M. H. Giacomoni, "Receding Horizon Control for Drinking Water Networks: The Case for Geometric Programming," *IEEE Transactions on Control of Network Systems*, vol. 7, no. 3, pp. 1151-1163, Sept. 2020. DOI: 10.1109/TCNS.2020.2964139.

[6] M.K. Singh, and V. Kekatos, "Optimal Scheduling of Water Distribution Systems," *IEEE Transactions on Control of Network Systems*, vol. 7, no. 2, pp. 711-723, June 2020. DOI: 10.1109/TCNS.2019.2939651.

[7] -, "EU Reference Document Good Practices on Leakage Management WFD CIS WG PoM", Main Report, 2015. DOI: 10.2779/102151.

[8] A.O. Lambert, "Water losses management and techniques," *Water Supply*, vol. 2, no. 4, pp. 1-20, 2002. DOI: 10.2166/ws.2002.0115.

[9] M. Tabesh, A.H.A. Yekta, and R. Burrows, "An Integrated Model to Evaluate Losses in Water Distribution Systems," *Water Resour Manage*, vol. 23, pp. 477–492, 2009. DOI: 10.1007/s11269-008-9284-2.

[10] M. Vermersch, F. Carteado, A. Rizzo, E. Johnson, F. Arregui, and A. Lambert, "Guidance Notes on Apparent Losses and Water Loss Reduction Planning", MCAST - Malta College of Arts Science and Technology, 2016. https://www.mcast.edu.mt/

[11] R. Pérez, V. Puig, J. Pascual, A. Peralta, E. Landeros, and Ll. Jordanas, "Pressure sensor distribution for leak detection in Barcelona water distribution network," *Water Supply*, vol. 9, no. 6, pp. 715-721, 2009. DOI: 10.2166/ws.2009.372.

[12] R. Steffelbauer, M. Neumayer, M. Günther, and D. Fuchs-Hanusch, "Sensor Placement and Leakage Localization Considering Demand Uncertainties," *Procedia Engineering*, vol. 89, pp. 1160-1167, 2014. DOI: 10.1016/j.proeng.2014.11.242.

[13] V. Ghorbanian, B.W. Karney and Y. Guo, "Minimum Pressure Criterion in Water Distribution Systems: Challenges and Consequences," in Proc. World Environmental and Water Resources Congress 2015: Floods, Droughts, and Ecosystems, Austin, TX, USA, 2015, pp. 777–791. DOI:10.1061/9780784479162.072.

[14] T. Walski, W. Bezts, E.T. Posluszny, M. Weir, and B.E. Whitman, "Modeling leakage reduction through pressure control," *JournalAWWA*, vol. 98, no. 4, pp. 147-155, April 2006. DOI: 10.1002/j.1551-8833.2006.tb07642.x.

[15] A. Lambert, M. Fantozzi and J. Thornton, "Practical approaches to modeling leakage and pressure management in distribution systems – progress since 2005," in Proc. 12th International Conference on Computing and Control for the Water Industry, Perugia, IT, 2013.

[16] A. Campisano, C. Modica, S. Reitano, R. Ugarelli, and S. Bacherian, "Field-Oriented Methodology for Real-Time Pressure Control to Reduce Leakage in Water Distribution Networks," *Journal of Water Resources Planning and Management*, vol. 142, no. 12, 2016. DOI: 10.1061/(ASCE)WR.1943-5452.0000697.

[17] M. Nicolini and L. Zovatto, "Optimal Location and Control of Pressure Reducing Valves in Water Networks," *Journal of Water Resources Planning and Management*, vol. 135, no. 3, 2009. DOI: 10.1061/(ASCE)0733-9496(2009)135:3(178).

[18] J.M. Grosso, C. Ocampo-Martinez, and V. Puig, "A distributed predictive control approach for periodic flow-based networks: application to drinking water systems," *International Journal of Systems Science*, vol. 48, no. 14, pp. 3106-3117, 2017. DOI: 10.1080/00207721.2017.1367051.

[19] F.K. Pour, V. Puig, and G. Cembrano, "Health-aware LPV-MPC Based on System Reliability Assessment for Drinking Water Networks," in Proc. IEEE Conference on Control Technology and Applications, Copenhagen, DK, 2018, pp. 577–582. DOI: 10.1109/CCTA.2018.8511348.

[20] Y. Wang, V. Puig, and G. Cembrano, "Non-linear economic model predictive control of water distribution networks," *Journal of Process Control*, vol. 56, pp. 23-34, 2017. DOI: 10.1016/j.jprocont.2017.05.004.

[21] Y. Wang, C. Ocampo-Martinez, and V. Puig, "Stochastic model predictive control based on gaussian processes applied to drinking water networks," *IET Control Theory Appl.*, vol. 10, no. 8, pp. 947–955, 2016. DOI: 10.1049/iet-cta.2015.0657

[22] M. Fantozzi, and A. Lambert, "Recent developments in pressure management," in Proc. IWA Int. Specialized Conf. Leakage, The Hague, NH, 2010.

[23] M. Girard, and R.A. Stewart, "Implementation of pressure and leakage management strategies on the Gold Coast, Australia: case study," *Journal of Water Resources Planning and Management*, vol. 133, no. 3, pp. 210–217, 2007. DOI: 10.1061/(ASCE)0733-9496(2007)133:3(210).

[24] S.M. Zanoli, G. Astolfi, L. Orlietti, M. Frisinghelli and C. Pepe, "Water Distribution Networks Optimization: a real case study", *IFAC-PapersOnLine*, vol. 53, no. 2, pp. 16644-16650, 2020. DOI: 10.1016/j.ifacol.2020.12.794.

[25] HR Wallingford, http://www.hrwallingford.it/software/infoworks-ws

[26] E. Creaco, A. Campisano, N. Fontana, G. Marini, P.R. Page and T. Walski, "Real time control of water distribution networks: A state-of-the-art review," *Water Research,* vol. 161, pp. 517-530, 2019. DOI: 10.1016/j.watres.2019.06.025.

[27] S. M. Zanoli and C. Pepe, "The importance of cooperation and consistency in two-layer Model Predictive Control," 17th International Carpathian Control Conference (ICCC), 2016, pp. 825-830. DOI: 10.1109/CarpathianCC.2016.7501210.

[28] S.M. Zanoli and C. Pepe, "Two-Layer Linear MPC Approach Aimed at Walking Beam Billets Reheating Furnace Optimization," *Journal of Control Science and Engineering*, Article ID 5401616, 15 pages, 2017, DOI: 10.1155/2017/5401616.

[29] C. Pepe and S. M. Zanoli, "A two-layer model predictive control system with adaptation to variables status values," 17th International Carpathian Control Conference (ICCC), 2016, pp. 573-578. DOI: 10.1109/CarpathianCC.2016.7501162.

[30] E. J. Davison and W. Smith, "Pole assignment in linear time-invariant multivariable systems with constant disturbances," *Automatica*, vol. 7, pp. 489-498, 1971. DOI: 10.1016/0005-1098(71)90099-9.

[31] B. A. Francis and W. M. Wonham, "The internal model principle of control theory," *Automatica*, vol. 12, pp. 457-465, 1976. DOI: 10.1016/0005-1098(76)90006-6.

[32] K. R. Muske and T. A. Badgwell, "Disturbance modeling for offset-free linear model predictive control," *Journal of Process Control*, vol. 12, pp. 617-632, 2002. DOI: 10.1016/S0959-1524(01)00051-8.

[33] G. Pannocchia and J.B. Rawlings, "Disturbance models for offset-free model predictive control," *AIChE Journal*, vol. 49, pp. 426-437, 2003. DOI: 10.1002/aic.690490213.

[34] J. Maciejowski, "Predictive Control with Constraints", *Prentice Hall*, 2002.

[35] M. D'Ercole, M. Righetti, G.S. Raspati, P. Bertola, and R.M. Ugarelli, "Rehabilitation Planning of Water Distribution Network through a Reliability-Based Risk Assessment," *Water*, vol. 10, no. 3, 2018. DOI: 10.3390/w10030277.

[36] J. Morrison, "Managing leakage by district metered areas: a practical approach," *Water*, vol. 21, pp. 44-46, 2004.

[37] J. Morrison, S. Tooms, and D. Rogers, "DMA Management Guidance Notes," *IWA Publication*, 2007.

[38] E. Creaco, D. Castagnolo and G. Pezzinga, "Assessing the Impact of Partitioning on Optimal Installation of Control Valves for Leakage Minimization in WDNs," *Water*, vol. 13, no. 7, 2021. DOI: 10.3390/w13071003.

[39] E. Creaco and H. Haidar, "Multiobjective Optimization of Control Valve Installation and DMA Creation for Reducing Leakage in Water Distribution Networks," *Journal of Water Resources Planning and Management*, vol. 145, no. 10, 2019. DOI: 10.1061/(ASCE)WR.1943-5452.0001114.

[40] L. Ljung, "System Identification. Theory for the User", *Prentice-Hall PTR*, 1999.

[41] B. De Schutter, "Minimal state-space realization in linear system theory: An overview," *Journal of Computational and Applied Mathematics, Special Issue on Numerical Analysis in the 20th Century – Vol. I: Approximation Theory*, vol. 121, no. 1–2, pp. 331–354, Sept. 2000.

[42] A. Bemporad, M. Morari, and N. Ricker, "Model Predictive Control Toolbox", 2005.

Silvia Maria Zanoli received an M. Sc. degree in Electronic Engineering in 1992 and a Ph.D. degree from the University of Ancona, Italy in 1996. She is currently an assistant professor at the Università Politecnica Marche, Italy, holding courses on the field of Industrial Automation. She has been visiting professor at the MSEL of the Northeastern University of Boston. She actually works on the development of advanced process control systems and fault diagnosis systems. Her research interests include model predictive control, advanced process control, fault-diagnosis, and supervision both on time-driven systems and on discrete event systems. She has collaborated on many national and European projects on robotics and industrial automations. Dr. Zanoli is a member of IEEE and of ISME (Interuniversity Center of Integrated Systems for the Marine Environment).

Crescenzo Pepe received a B.Sc. and an M.Sc. degrees in Computer and Automation Engineering from Università Politecnica delle Marche, in 2010 and 2013. He received a Ph.D. degree (2017) in Information Engineering from the same university, working with a company. He was professor at a secondary school and a high school. He was a control/automation engineer/researcher in different companies. He was one of the inventors (research, development, publications, patents, application to real case studies, project management and maintenance, technical coordination and supervision, training of internal and external resources) of many advanced process control solutions for industrial and non-industrial processes. He has developed more than 20 advanced process control projects and he is co-author of more than 40 scientific publications and of an Italian patent. Currently he is a Postdoctoral Research Fellow at Università Politecnica delle Marche. His main interests are control theory and applications and industrial automation.

Giacomo Astolfi received a B.Sc. and an M.Sc. degrees in Automation Engineering from Università Politecnica delle Marche, in 2006 and 2009. He received a Ph.D. degree (2012) in Engineering Science, "Computer, management and automation engineering" curriculum, from the same university. Currently he is Head of Innovation IoT & New Business at Alperia Green Future.

Lorenzo Orlietti received a B.Sc. and an M.Sc. degrees in Automation Engineering from Università Politecnica delle Marche, in 2008 and 2011. He received a Ph.D. degree (2015) in Engineering Science, "Computer, management and automation engineering" curriculum, from the same university. Currently he is Head of Engineering Sybil Industrial at Alperia Green Future - Innovation IoT & New Business.